J|A|C|S
ARTICLES
Published on Web 11/22/2003

Probing Chiral Selective Reactions Using a Revised Kataura Plot for the Interpretation of Single-Walled Carbon Nanotube Spectroscopy

Michael S. Strano*

Contribution from the Department of Chemical and Biomolecular Engineering, University of Illinois at Urbana/Champaign, Urbana, Illinois 61801

Received June 19, 2003; E-mail: strano@uiuc.edu

Abstract: Raman spectroscopy on surfactant-dispersed, aqueous suspensions of single-walled carbon nanotubes is used to verify the energies of interband transitions and validate the spectral assignments of semiconducting and metallic nanotubes determined by spectrofluorimetry for the former and Raman excitation profiles for the latter. The results are compiled into an experimentally based mapping of transition versus nanotube diameter to revise those previously employed using single-electron theoretical treatments. Because this mapping provides the transitions associated with a precise chiral wrapping of a particular nanotube, it allows the monitoring of reaction pathways that are selective to the nanotube chirality vector. This is demonstrated using a model electron-transfer reaction of 4-chlorobenzenediazonium shown to be selective for metallic over semiconducting carbon nanotubes via charge-transfer stabilization of complexes at the surfaces of the former.

Introduction

Carbon nanotubes are an important class of materials for the development of novel electronic and optical devices, field emission electrodes, as well as elements of polymer composites.[1−3] Recent advances in the solution phase dispersion,[4] spectroscopic detection,[5] and spectral assignments[6,7] of single-walled carbon nanotubes give researchers new tools to probe and understand their surface reactions with unprecedented detail. The remaining task is to link reaction pathways and sidewall chemistries to the unique electronic structure of these materials.

This unique electronic structure arises from the quantinization of the electronic wave vector of the 1-D system through the conceptual rolling of a graphene plane into a cylinder forming the nanotube. The vector in units of hexagonal elements connecting two points on this plane defines the nanotube chirality in terms of two integers: n and m.[1,3] When $|n - m| = 3q$ where q is an integer, the nanotube is metallic or semimetallic while remaining species are semiconducting with a geometry-dependent band gap. Raman spectroscopy has been used extensively to characterize solid[8] and solution phase[4] carbon nanotube systems because it has the ability to probe distinct populations of nanotubes that have interband transitions in resonance with the excitation laser. Low wavenumber phonon modes[9]—radial breathing modes (RBMs)—have Raman shifts strongly dependent on nanotube diameter.[10] In this way, nanotubes of a distinct chiral vector can be identified and tracked during chemical processing, yielding new insight into nanotube surface chemistry.

The interpretation of nanotube fluorescence,[7] absorption,[5] and Raman spectroscopy[8,9,11] is highly dependent on an understanding of this electronic structure. The original organization of electronic transitions of carbon nanotubes as a function of their diameter is attributed to H. Kataura.[12] Here, the Tight Binding Approximation was used to describe carbon nanotube electronic structure as that of a graphene sheet with electronic wavevectors quantized into distinct integer multiples.[13] The formalism predicts the organization of metallic and semiconducting transitions based on the chirality vector. Real nanotube structure is complicated from this simplified approximation due to a number of effects: trigonal warping or the warping of the Brillion zone due to curvature[14] introduces deviations, other curvature effects the change circumferential bond lengths,[3] and orbital overlap

(1) Dresselhaus, M. S.; Dresselhaus, G.; Eklund, P. C. *Science of Fullerenes and Carbon Nanotubes*; Academic Press: San Diego, CA, 1996.
(2) Avouris, P. *Acc. Chem. Res.* **2002**, *35*, 1026−1034.
(3) Saito, R.; Dresselhaus, G.; Dresselhaus, M. S. *Physical Properties of Carbon Nanotubes*; Imperial College Press: London, 1998.
(4) Strano, M. S.; Moore, V. C.; Miller, M. K.; Allen, M. J.; Haroz, H. A.; Kittrell, C.; Hauge, R. H.; Smalley, R. E. *J. Nanosci. Nanotechnol.* **2003**, *3* (1-2), 81−86.
(5) O'Connell, M. J.; Bachilo, S. M.; Huffman, C. B.; Moore, V. C.; Strano, M. S.; Haroz, E. H.; Rialon, K. L.; Boul, P. J.; Noon, W. H.; Kittrell, C.; Ma, J. P.; Hauge, R. H.; Weisman, R. B.; Smalley, R. E. *Science* **2002**, *297*, 593−596.
(6) Strano, M. S. *Nano Lett.* **2003**, *3*, 1379-1382.
(7) Bachilo, S. M.; Strano, M. S.; Kittrell, C.; Hauge, R. H.; Smalley, R. E.; Weisman, R. B. *Science* **2002**, *298*, 2361−2366.
(8) Kukovecz, A.; Kramberger, C.; Georgakilas, V.; Prato, M.; Kuzmany, H. *Eur. Phys. J. B* **2002**, *28*, 223−230.
(9) Dresselhaus, M. S.; Dresselhaus, G.; Jorio, A.; Souza, A. G.; Saito, R. *Carbon* **2002**, *40*, 2043−2061.
(10) Sauvajol, J. L.; Anglaret, E.; Rols, S.; Alvarez, L. *Carbon* **2002**, *40*, 1697−1714.
(11) Yu, Z. H.; Brus, L. E. *J. Phys. Chem. A.* **2000**, *104*, 10995−10999.
(12) Kataura, H.; Kumazawa, Y.; Maniwa, Y.; Umezu, I.; Suzuki, S.; Ohtsuka, Y.; Achiba, Y. *Synth. Met.* **1999**, *103*, 2555−2558.
(13) Mintmire, J. W.; White, C. T. *Phys. Rev. Lett.* **1998**, *81*, 2506−2509.
(14) Saito, R.; Dresselhaus, G.; Dresselhaus, M. S. *Phys. Rev. B* **2000**, *61*, 2981−2990.

10.1021/ja036791x CCC: $25.00

that introduces influences from multiple neighbors[15] in the carbon lattice causing a breakdown of the Tight Binding Approximation. Moreover, these single electron models cannot describe multiple electron influences, such as exciton interactions, and this also complicates the comparison between theory and experiment.[16,17] As a consequence, past efforts to assign the spectral features of carbon nanotubes that have relied on theoretical-based mappings have had limited success.[5,7]

This work underscores this point by using Raman spectroscopy with a range of excitation wavelengths to compare the observed spectra to an experimentally produced mapping of energetic transitions. We show the utility of such a spectral assignment using a model electron-transfer reaction in which 4-chlorobenzenediazonium is shown to selectively react with metallic carbon nanotubes over semiconducting ones as determined by Raman spectroscopy. Previous work has shown that solution phase protonation[18] of single-walled carbon nanotubes is highly selective depending upon the nanotube band gap. The charge transfer in this reversible, noncovalent interaction opens the possibility for covalent, irreversible pathways to show analogous selectivity. This possibility is explored more fully in this work.

Experimental Section

Sample Preparation. HiPco[19] carbon nanotubes (reaction #89) from Rice University were suspended in sodium dodecyl sulfate (SDS) (Sigma Aldrich) using a method reported previously.[5,18] Briefly, 1 wt % surfactant was combined with 40 mg of nanotube material in 200 mL of water and ultrasonicated at 590 W for 10 min after high shear mixing for 1 h. The suspension was centrifuged for 4 h at 200000g using a swing bucket rotor after which the decant was isolated and used for subsequent experiments.

Raman Spectroscopy. Samples were characterized in solution by transferring to a quartz cuvette. Raman spectroscopy was performed at 532 and 785 nm (2.33 and 1.58 eV) excitations using a Kaiser Optical RXN1 spectrometer at 10× magnification with 32 and 100 mW at the sample for each wavelength, respectively. Spectra generated at 633 and 830 nm (1.96 and 1.50 eV) were obtained using a setup from Renishaw fitted with a macroscopic sampling kit, a 50× (long) objective, and approximately 15 mW of power at the sample. Spectroscopic grade cyclohexane (Sigma Aldrich) was used in the same geometric configuration as an intensity calibration standard.[20] Each Raman spectrum in the region from 175 to 400 cm^{-1} was fitted using a summation of Lorentzian peak shapes.

Selective Reaction. Reagents and solvents to synthesize 4-chlorobenzenediazonium were obtained from Sigma Aldrich. This reagent was stored under N_2 and at −2 °C until use. Reaction was carried out in a stirred vessel containing the carbon nanotube suspension to which a metered amount of 4-chlorobenzenediazonium in aqueous solution was added to yield the desired ratio of reagent to nanotube concentration. The pH of the nanotube solution was kept constant at approximately 10 using an addition of NaOH to avoid spectral behavior associated with protonation.[18] Raman spectroscopy was performed on the reaction mixture using the method described above with successive spectra taken to indicate when the steady state was reached.

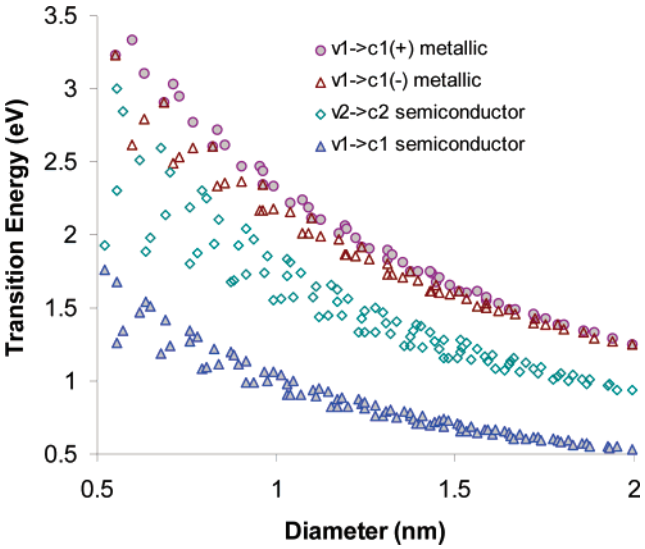

Figure 1. Experimentally compiled plot of interband transitions versus diameter for metallic and semiconducting single-walled carbon nanotubes. The former split into high (+)- and low (−)-energy transitions.

Results and Discussion

A Revised, Experimental Kataura Plot. In previous work by Kukovecz and co-workers,[8] the Raman spectra of solid carbon nanotube ropes have been examined in detail. Roped nanotubes develop an orthogonal dispersion in their otherwise 1-D electronic structure, and this significantly perturbs the energetics of pristine nanotube interband transitions.[21] This work circumvents this pitfall by using surfactant-assisted dispersion, which provides a spectroscopically homogeneous environment for optical measurements.[4]

While variations of the Kataura plot have been widely used in the interpretation of experiments,[8−10,22] there is growing evidence that experimentally determined interband transitions cannot be described by theoretical models of electronic structure.[16,17] For semiconductors, spectrofluorimerty has been used to map the interband transitions upon excitation from the valence (v) to the conduction (c) bands denoted vn → cn, where n is the band index. Sizable deviations from the conventional Kataura plot have been noted.[7] Also, separate Raman excitation profiles of nanotubes in the metallic absorbing region have been used to map the v1 → c1 transitions of the metallic nanotubes.[6] These transitions have been correlated using semiempirical expressions derived from asymptotic expansions in diameter of the electron dispersion relation for graphene. The reader is also referred to the Supporting Information that contains a useful compilation of these data.

These results are compiled for the reader into an experimental Kataura plot for the interpretation of optical experiments involving single-walled carbon nanotubes. Figure 1 presents the plot for nanotubes up to 2 nm in diameter for the first and second interband transitions of the semiconductors and the first transitions of the metallic and semimetallic nanotubes. The latter split into high- and low-energy transitions for nonarmchair ($n \neq m$) metallic nanotubes[13,14,23] (actually semimetallic due to a curvature-

(15) Reich, S.; Maultzsch, J.; Thomsen, C.; Ordejon, P. *Phys. Rev. B* **2002**, *66*, 035412.
(16) Ando, T. *J. Phys. Soc. Jpn.* **1997**, *66*, 1066−1073.
(17) Keane, M.; Mele, E. J. *Phys. Rev. Lett.* **2003**, *90*, No. 207401.
(18) Strano, M. S.; Huffman, C. B.; Moore, V. C.; O'Connell, M. J.; Haroz, E. H.; Hubbard, J.; Miller, M.; Rialon, K.; Kittrell, C.; Ramesh, S.; Sivarajan, R.; Hauge, R. H.; Smalley, R. E. *J. Phys. Chem. B* **2003**, *107*, 6979−6985.
(19) Bronikowski, M. J.; Willis, P. A.; Colbert, D. T.; Smith, K. A.; Smalley, R. E. *J. Vac. Sci. Technol.* **2001**, *19*, 1800−1805.
(20) McCreery, R. L. *Photometric Standards for Raman Spectroscopy*; John Wiley & Sons: Chichester, U.K., 2002.
(21) Reich, S.; Thomsen, C.; Ordejon, P. *Phys. Rev. B* **2002**, *65*, 155411.
(22) Yu, Z. H.; Brus, L. E. *J. Phys. Chem. B* **2001**, *105*, 6831−6837.

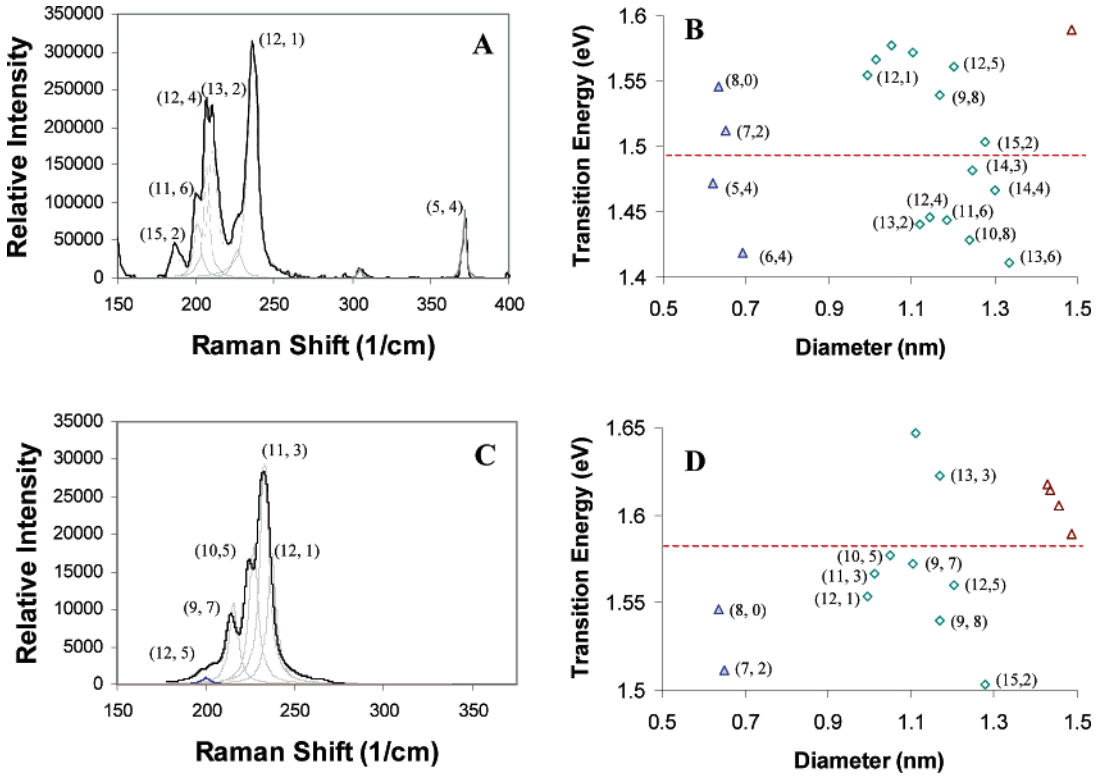

Figure 2. Low wavenumber Raman shift spectrum for a solution of suspended carbon nanotubes at (A) 830 nm excitation with (B) a comparison to the data in Figure 1. In (C) the spectrum is generated at 785 nm excitation and also (D) compared in a similar manner.

induced electronic gap.) When compared to its widely used, theoretically based analogue, this mapping reveals that there is a greater deviation from the "armchair curve": a limiting inverse diameter curve that provides the limit of the transition energy as diameter goes to infinity. At small diameters, transitions are significantly intermixed, in marked contrast to the predictions of single electron treatments. This intermixing is of some utility in probing selective reaction chemistries as detailed below.

Probing Nanotube Chirality and Electronic Type Using Raman Spectroscopy. Figure 1 can be used to predict which nanotubes are in resonance at a particular excitation wavelength using Raman spectroscopy. The RBMs[3,9] in this spectrum have been shown to follow the relationship[8]

$$\omega_{\mathrm{RBM}} = A + \frac{B}{d_t}$$

where A is 223.5 nm cm^{-1} and B is 12.5 cm^{-1} for HiPco samples under these conditions.[6,7] Figure 1 can be used with eq 1 to predict which RBM features will be apparent at a particular excitation wavelength. This is demonstrated in Figure 2a for single-walled carbon nanotubes suspended in aqueous solution. At 830 nm, the Kataura plot predicts resonance with the v2 → c2 transitions of a cluster of semiconducting nanotubes and the v1 → c1 transition of one small diameter species (5,4). Figure 2b compares the deconvoluted Raman spectrum with an expanded version of the plot in Figure 1 using eq 1 to rescale the diameter axis in terms of Raman shift of the RBM feature. The mapping is able to predict the Raman shift associated with each (n,m) nanotube and the transition within the resonance window (40 meV) of the excitation laser.[6,7]

Figure 2, parts c and d, provides this same comparison for the Raman spectrum at 785 nm (1.58 eV) excitation. Here, semiconducting nanotubes excited at their v2 → c2 transitions are observed exclusively. Excellent agreement is observed between the predicted and experimental spectral features. At 633 nm excitation (Figure 3a), we probe a gap between transitions with some large diameter metallic nanotubes resonant and five semiconducting nanotubes at smaller diameters that are also present. This wavelength is particularly instructive for researchers inquiring about metal and semiconductor separation[24−26] or chemistries selective to particular electronic types as demonstrated in this work. Figure 3b demonstrates the ability to describe this transition region with high accuracy. Figure 3c at 532 nm (2.33 eV) probes mostly the v1 → c1 of metallic nanotubes with the exception of one or two small diameter semiconductors present: (9,2) or (10,0). These last nanotubes have been confirmed to be, in fact, large band gap semiconductors using selective protonation[18] in solution, and this provides excellent agreement with the revised plot. The comparison between predicted and observed transitions is acceptable, although several metallic features are only partially resonant (Figure 3d).

Probing Selective Chemical Interactions with Carbon Nanotubes. In the investigation of nanotube surface chemistries, the utility of the spectral assignments and the mapping provided in this work is that particular (n,m) interactions can now be understood more thoroughly. For example, covalent attachment of moieties at the sidewall of a carbon nanotube disrupts the

(23) Reich, S.; Thomsen, C. *Phys. Rev. B* **2000**, *62*, 4273−4276.
(24) Krupke, R.; Hennrich, F.; von Lohneysen, H.; Kappes, M. M. *Science* **2003**, *301*, 344−347.
(25) Zheng, M.; Jagota, A.; Strano, M. S.; Semke, E. D.; Mclean, R. S.; Onoa, G. B.; Walls, D. J. *Nature*, submitted for publication, 2003.
(26) Chattopadhyay, D.; Galeska, I.; Papadimitrakopoulos, F. *J. Am. Chem. Soc.* **2003**, *125*, 3370−3375.

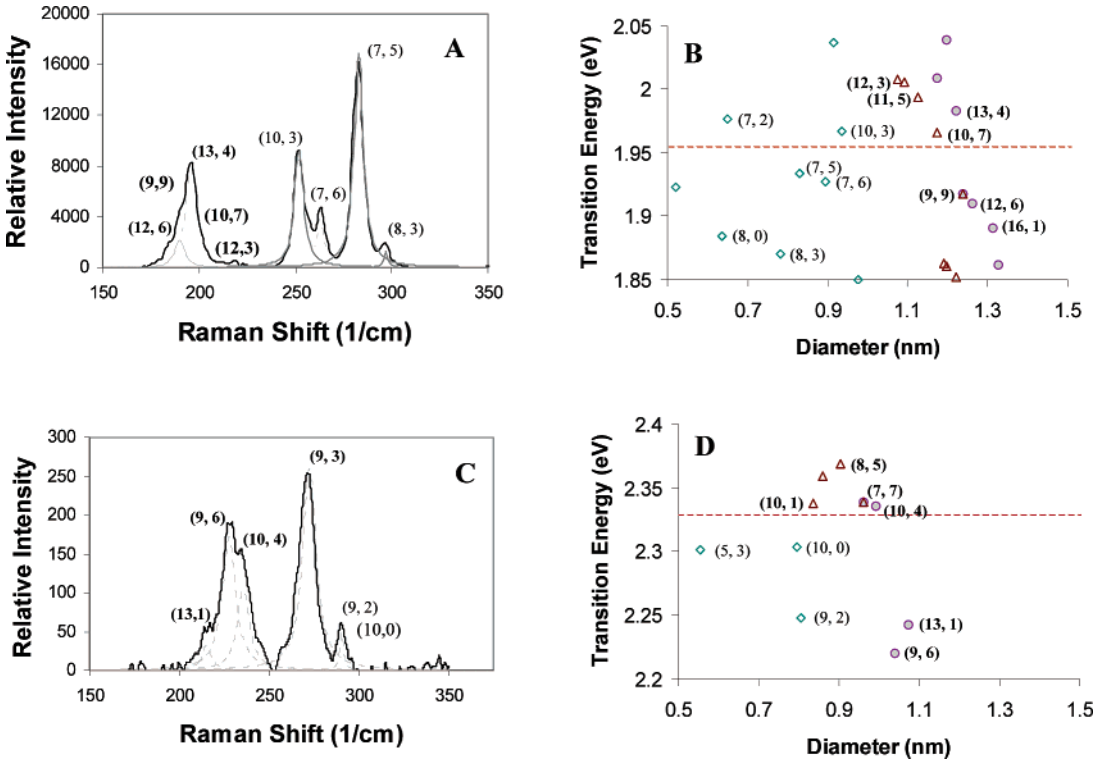

Figure 3. Low wavenumber Raman shift spectrum for a solution of suspended carbon nanotubes at (A) 633 nm excitation with (B) a comparison to the data in Figure 1. In (C) the spectrum is generated at 532 nm excitation and also (D) compared in a similar manner.

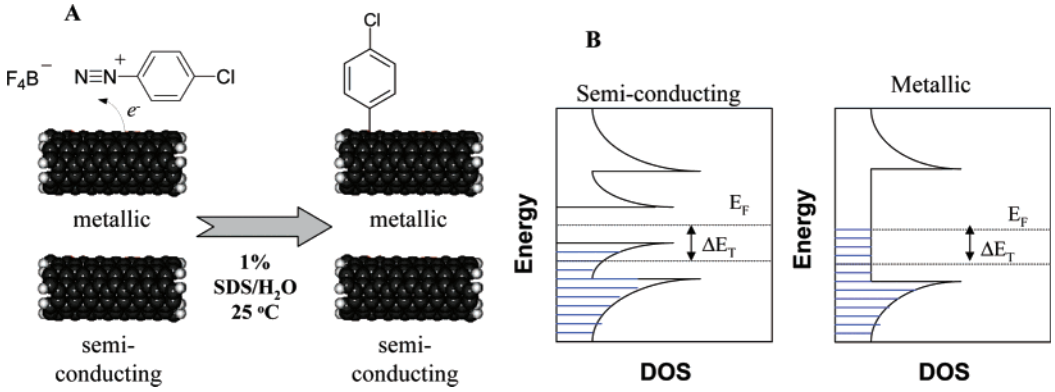

Figure 4. The nanotube transfers an electron (A) with a rate that depends on the electronic characteristics of the nanotube. (B) Electron transfer depends on the density of states in that electron density; ΔE_F, near the Fermi level translates into higher reactivity for metallic over semiconducting nanotubes.[32]

symmetry of the Raman radial mode, and this (*n*,*m*)-dependent feature decays accordingly.[27−29] Conversely, adsorbates that localize electrons on the nanotube surface diminish Raman resonance enhancement but leave this phonon mode intact.[30] This alone has the power to differentiate covalent from noncovalent chemistries for particular (*n*,*m*) nanotubes. This distinguishes Raman spectroscopy from XPS on the reacted surface, NMR on the proposed reagent, AFM, and TEM. These techniques cannot yield this information despite their exclusive, widespread employment to characterize carbon nanotube chemistry.

An important example of chiral selectivity in carbon nanotube functionalization is the case of diazonium salts.[27−29] These reagents extract electrons from nanotubes in the formation of a covalent aryl bond (Figure 4a), and we find that under controlled conditions they do so selectively with metallic to the exclusion of the semiconducting nanotubes. This bond forms with high affinity for electrons with energies near the Fermi level of the nanotube (Figure 4b). The reactant participates in a charge-transfer complex at the surface with electron donation stabilizing the transition state.

This behavior can be exploited to obtain highly selective functionalization of metallic and semimetallic nanotubes to the exclusion of the semiconductors. As suggested by Figure 4a,b, Raman spectroscopy at 633 nm (1.96 eV) excitation is ideal for probing these selective interactions because of its resonance with a population of metallic and semiconducting nanotubes for material synthesized by the HiPco method.[19] Figure 5 shows the Raman spectrum of an aqueous dispersion of carbon nanotubes with increasing additions of 4-chlorobenzenediazo-

(27) Bahr, J. L.; Tour, J. M. *J. Mater. Chem.* **2002**, *12*, 1952−1958.
(28) Bahr, J. L.; Yang, J.; Kosynkin, D. V.; Bronikowski, M. J.; Smalley, R. E.; Tour, J. M. *J. Am. Chem. Soc.* **2001**, *123*, 6536−6542.
(29) Dyke, C. A.; Tour, J. M. *J. Am. Chem. Soc.* **2003**, *125*, 1156−1157.
(30) Itkis, M. E.; Niyogi, S. E.; Meng, M. E.; Hamon, M. A.; Hu, H.; Haddon, R. C. *Nano Lett.* **2002**, *2*, 155−159.

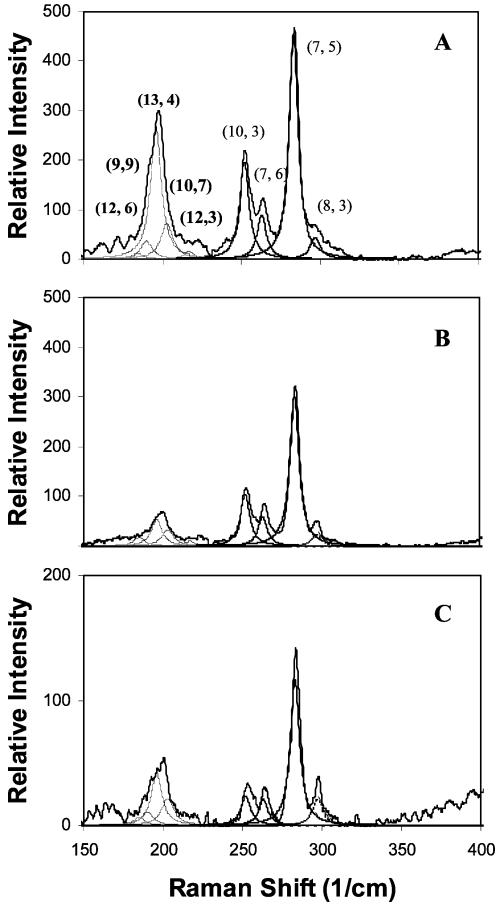

Figure 5. Selective reaction at 633 nm Raman excitation. The spectrum probes large diameter metallic nanotubes and smaller diameter semiconductors. As the conversion increases upon subsequent metered additions of reagent (measured as mol reagent/mol 1000 carbon), features assigned to metallic nanotubes react first. (A) 0, (B) 18.6, and (C) 29.1 groups/1000 mol.

nium normalized as mol of reagent per 1000 mol of carbon atoms in the system. At low conversion (18 side groups per 1000 carbons), the radial phonon modes of the metallic nanotubes decay to the near exclusion of the semiconductors. The preservation of the band gap fluorescence of the latter confirms the reaction selectivity since nanotube emission is known to be highly sensitive to sidewall, chemical defects that disrupt symmetry. The selective, complete decay of these modes associated with metallic species identifies this process as distinct from reversible electronic withdraw or "doping" processes.[30]

The functionalization increases the intensity of a phonon mode at 1330 cm^{-1} in the Raman spectrum. Its presence indicates the formation of an sp^3 C−sp^2 C nanotube−aryl bond. The functionalization disrupts the radial phonon that gives rise to low-frequency Raman lines distinct for species of a particular diameter which causes the mode to decay accordingly as the particular (*n*,*m*) nanotube reacts. Figure 6 is the Raman spectrum at 532 nm (2.33 eV) showing the relative rates of the decays of various metallic species.[31] Low-frequency Raman modes assigned to the (9,2) and (10,0) semiconductors remain unaffected when all v1 → c1 transitions of semimetallic and metallic species in the sample have decayed. This provides excellent

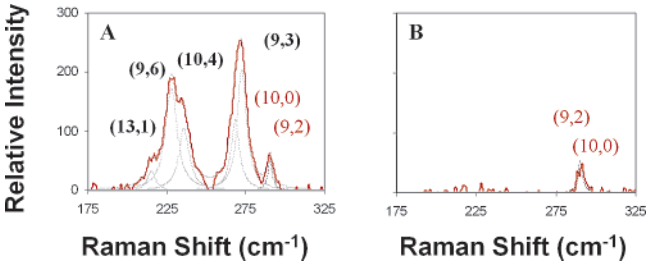

Figure 6. (A) Similar low wavenumber spectrum at 532 nm excitation of the prepared solution. Four metallic nanotubes and one semiconductor (red) are probed. (B) After a ratio of 22.4, all metallic modes have decayed, leaving only the single semiconductor in agreement. Increasing the reaction extent results in the functionalization of this last species as well.[31]

agreement with Figure 3a. Absorption spectra taken on the reacted and unreacted samples are also consistent with the selective functionalization of carbon nanotubes for species in the HiPco diameter range (see Supporting Information).

A revised Kataura plot as presented in Figure 1 can be used in this way as a more effective gauge of reaction chemistry, particularly those reaction pathways that favor an electronic type such as in charge-transfer complexation or those that favor smaller diameters such as surface oxidations[32] or particularly nitric acid treatments.[30] In recent efforts attempting to demonstrate the separation of carbon nanotubes by their electronic type, the analysis was limited by the inaccuracy in the correlation of transition energies with diameter that was used in the interpretation of spectra at 785 nm (1.58 eV) and 514.5 nm (2.41 eV). Several researchers use the inverse diameter limits derived from Saito and co-workers from a Tight Binding Formalism with trigonal warping correction[14,23] in spite of its limited applicability to situations where the norm of the *k*-vector is small and the dispersion relation can be linearized. The actual mapping (Figure 1) has been experimentally verified for both the small and large diameter limits and can identify wavelengths, highlighted in this work, that are in resonance with both metals and semiconductors. These wavelengths are particularly valuable for gauging metal and semiconductor separation in a manner similar to the monitoring of selective chemical interactions (Figure 6).

Conclusions

Raman spectroscopy is used to validate the correlation of single-walled carbon nanotube interband transitions with the radial breathing modes of distinct, chiral nanotubes. The results are compiled in a mapping of transitions versus diameter to replace theoretically based analogues that are widely employed in the interpretation of nanotube-related experiments. This experimentally based mapping allows researchers, for the first time, to track selective reaction pathways of particular carbon nanotubes. This is demonstrated by examining the changes in the Raman spectrum at 633 and 532 nm (1.96 and 2.33 eV) excitation after addition of 4-chlorobenzenediazonium, a species known to form a strong charge-transfer complex at the nanotube surface. The stability of this complex is dependent upon the characteristics of electron donation of a particular nanotube and, hence, favors metallic species over semiconducting ones. This mapping should also provide assistance to efforts attempting

(31) Strano, M. S.; Dyke, C. A.; Usrey, M. L.; Barone, P. W.; Allen, M. J.; Shan, H.; Kittrell, C.; Hauge, R. H.; Tour, J. M.; Smalley, R. E. *Science* **2003**, *301*, 1519−1522.

(32) Zhou, W.; Ooi, Y. H.; Russo, R.; Papanek, P.; Luzzi, D. E.; Fischer, J. E.; Bronikowski, M. J.; Willis, P. A.; Smalley, R. E. *Chem. Phys. Lett.* **2001**, *350*, 6−14.

to sort or separate carbon nanotubes according to their electronic type.

Acknowledgment. The author thanks C. Dyke and J. Tour at Rice University for many helpful discussions of diazonium reagents and carbon nanotube surface chemistry. R. B. Weisman is especially thanked for useful insights into carbon nanotube electronic structure. Research-grade HiPco nanotubes were supplied as a gift from the Smalley research group at Rice University. The author wishes to acknowledge financial support from the Molecular Electronics Group at the Dupont Co., Central Research and Development as well as from the Research Board of the University of Illinois at Urbana/Champaign.

Supporting Information Available: Tables of semiconductor and metallic transitions and figures of absorption spectra (PDF). This material is available free of charge via the Internet at http://pubs.acs.org.

JA036791X